VERY LARGE TELESCOPE

MACAO Lenslet Array Unit
Design Report

Doc. No.: VLT-TRE-ESO-11640-2451

Issue: 1.0

Date: 30.01.2001

Prepared:	M. Kasper, J. Farinato, A. Silber, R. Conzelmann, C. Dupuy, S. Tordo	30.01.01	
	Name	Date	Signature
Approved:	R. Arsenault	30.01.01	
	Name	Date	Signature
Released:	N. Hubin	30.01.01	
	Name	Date	Signature

CHANGE RECORD

ISSUE	DATE	SECTION/PARA. AFFECTED	REASON/INITIATION DOCUMENTS/REMARKS
1.0	30.01.2001	All	first issue

Table of Contents

1 ACRONYMS

AD	Applicable Document
AO	Adaptive Optics
AT	Auxiliary Telescope
APD	Avalanche Photo Diode
CWFS	Curvature Wavefront Sensor
CPS	Counts Per Second
DM	Deformable Mirror
ESO	European Southern Observatory
FOV	Field of View
HO	High Order
HW	Hardware
IR	Infrared (1.0-2.2µm)
LOS	Line of Sight, the seeing in the direction that the scope is looking
MACAO	Multiple Applications Curvature Adaptive Optics
Mas	Milli arcsec on the sky
MLM	Microlens Module
ND	Neutral Density filter
NGS	Natural Guide Star (a point source < 0.2" in size)
PSF	Point Spread Function
RD	Reference Document
SINFONI	SINgle Faint Object Near infrared Investigation
SOS	Super OS
STRAP	System for Tip-tilt Removal with Avalanche Photodiodes
SW	Software
TBC	To be confirmed
TBD	To be determined
UT	Unit Telescope (8.2-m diameter)
VLT	Very Large Telescope
VLTI	VLT Interferometer (1 – 13 µm)
WFS	Wavefront Sensor
WRT	with respect to

2 SCOPE

This design report presents a concept for the complete lenslet array unit and an analysis of the strong requirements for the alignment of the MACAO microlens module (MLM), a mechanical design to meet the tolerances, and an experiment to proof its design concept.

3 APPLICABLE DOCUMENTS

AD 1	*Top-Level Requirements for MACAO-VLTI*	VLT-SPE-ESO-15600-2082	Issue 1.2	01-09-00

4 REFERENCE DOCUMENTS

RD 1	*MACAO-VLTI Functional Requirements and operational concepts*	VLT-SPE-ESO-15600-2056	Issue 1.1	27.09.00
RD 2	*MACAO-VLTI System Design Overview*	VLT-TRE-ESO-15600-2251	Issue 1.1	27.09.00
RD 4	*MACAO-VLTI Wavefront Sensor Optics*	VLT-TRE-ESO-15600-2273	Issue 1.0	27.09.00
RD 5	*MACAO-VLTI Electronics - Overview*	VLT-TRE-ESO-15600-2268	Issue 1.0	27.09.00
RD 6	*MACAO-VLTI Software Functional Specifications – OS/ICS*	VLT-SPE-ESO-15600-2061	Issue 1.1	27.09.00
RD 7	*MACAO-VLTI Software VLTI Software Functional Specifications - RTC*	VLT-SPE-ESO-15600-2062	Issue 1.1	27.09.00
RD 8	*MACAO Technical Specifications and Statement of Work for the two Lenslet Arrays*	VLT-SPE-ESO-11640-2460	Issue 1.0	30.01.01
RD 9	*MACAO-VLTI VLTI Interface Control Document*	VLT-ICD-ESO-15600-2057	Issue 1.0	27.09.00
RD 10a	*MACAO technical specification and statement of work for the two micro lenslet arrays*	VLT-SPE-ESO-11640-2460	Issue 1.0	27.09.00
RD 10b	*Technical Specification for the MACAO WFS lenslet array units*	VLT-SPE-ESO-11640-2146	Issue 2.1	27.09.00
RD 11	*MACAO-VLTI Electronics – APD*	VLT-SPE-ESO-15600-2269	Issue 1.0	27.09.00
RD 12	*Technical Specification and Statement of Work for the MACAO Tip-Tilt Mount*	VLT-SPE-ESO-11640-2147	Issue 1.0	27.09.00
RD 13	*MACAO-VLTI Deformable Mirror: Technical Specification*	VLT-SPE-ESO-15600-2064	Issue 1.1	27.09.00
RD 14	*Technical Specification: ESO Adaptive Optics System: Deformable Mirror Control*	VLT-SPE-ESO-11640-1943	Issue 2.1	27.09.00
RD 15	*Technical specification: MACAO APD Counter module*	VLT-SPE-ESO-11640-2262	Issue 1.0	27.09.00
RD 16	*MACAO-VLTI technical specification: X-Y table.*	VLT-SPE-ESO-15600-2126	Issue 1.1	27.09.00
RD 17	*Assembly, integration and test plans for MACAO-VLTI*	VLT-PLA-ESO-15600-2241	Issue 1.0	27.09.00

5 INTRODUCTION

The development of the MLM (meaning with this term the complete system, starting with the first lenslet array and ending with the FC connector of the fibres) inside ESO has started at the beginning of October 2000, after realising that no contacted company was interested in manufacturing a complete system.

Using a single lenslet array to create spots on the fibers causes the following problem: each spot should be smaller than the fiber core of 100 μm, pushing the lenses composing the lenslet array towards fast f/numbers. Fast f/numbers in turn imply a small radius of curvature, i.e. large sag at the edges of the lenslets which most technologies used to produce lenslet arrays cannot handle with the required precision.

A possible solution would be to place another lens just in front of each fibre, thus relaxing the constraint on the f-ratio of the lenses composing the 1^{st} array. These additional lenses could image the lenslets of the 1^{st} array onto the fiber cores creating micro-pupils.

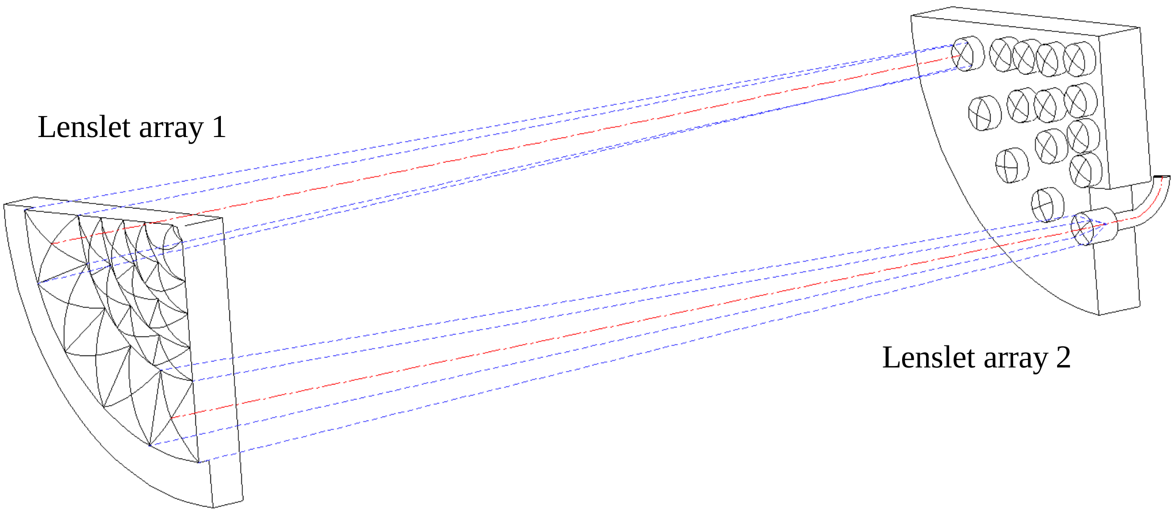

Figure 1: Overall view of the lenslet array unit: on the left ¼ of the first lenslet array, on the right ¼ of the second lenslet array and one fiber.

Figure 1 displays the key elements of the MLM, being:

- the first lenslet array with a typical CWFS keystone geometry.
- the second lenslet array that has the purpose to shrink the 60 spots (micropupils) coming from the first lenslet array and to feed them into the 60 fibres; basically, it is a mostly flat glass plate with 60 small circular lenslets of 0.7mm diameter placed at the position of the vertexes of the first lenslet array.
- the fibres housing, with three interface plates to ensure the correct alignment of the 60 fibres with the corresponding micropupils produced by the second lenslet array. The fibres housing further ensures the proper and safe guiding of the fragile fibers.

RD8 gives the technical specifications for both lenslet arrays and a statement of work.

6 OVERALL TOLERANCES OF THE LENSLET ARRAY UNIT

Considering that on the fibres the final image will be an image of the pupil of the first lenslet array, we made a computation of the losses of light produced by misalignments.

We computed the size of the lenses belonging to different rings of the first lenslet array. The largest microlenses are on the outer ring. Their size, when imaged by the second lenslet array, is comparable to the fiber core of diameter 100 µm. To simplify the computation, we considered a square shape for the lens. Figure 2 depicts the geometry. Please note that the assumption of a square actually produces larger losses of light than the real keystone shape. Furthermore, the largest subapertures (outer ring) are considered in this analysis representing the worst case.

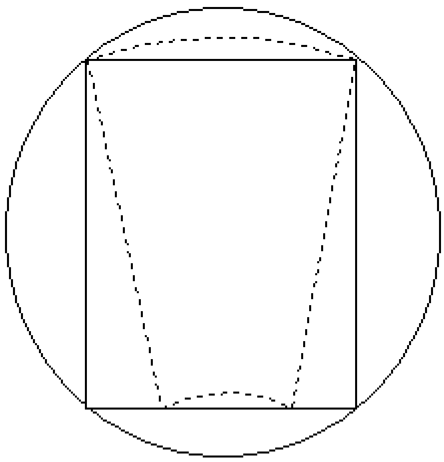

Figure 2: Real shape of the outer lens (dashed line) and considered shape (continuous line) inside the 100µm core fibre (external circle)

We considered three different directions for a total displacement of 10µm, and in the three cases we found a total loss of light of ~2% (see Figure 3).

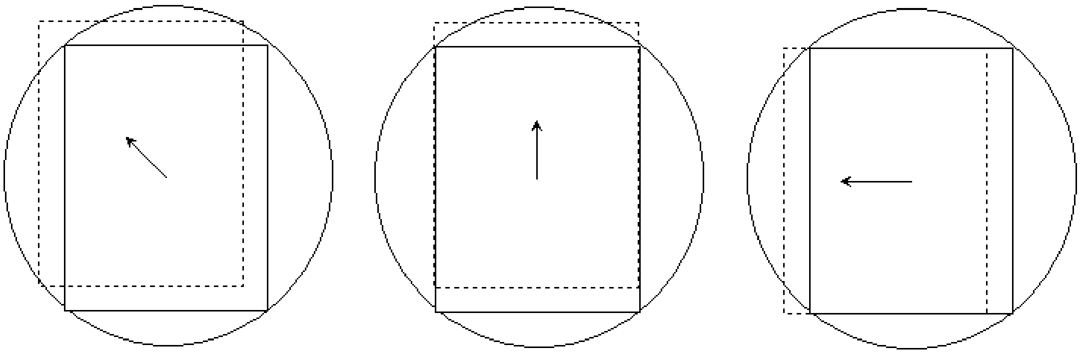

Figure 3: The three directions of the 10 µm displacement considered

There are **no losses** of light for a 10 µm displacement of the smaller lenses in the inner rings, and considering that in close loop the real shape of the pupil will be smaller than in open loop (see Figure 4), a 10 µm overall displacement as the goal for the tolerance specifications appears acceptable.

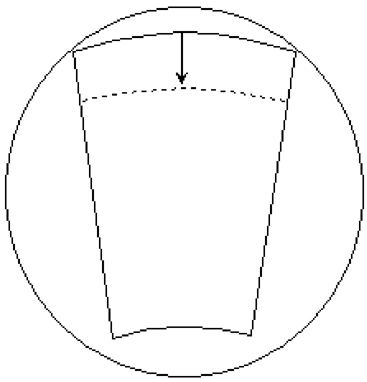

Figure 4: Shrinking of the pupil image tip-tilt is corrected. The outer ring subapertures are oversized to allow for tip-tilt correction.

6.1 Alignment tolerances

Perceiving that a mismatch in position of 10 µm between a micropupil and the respective fiber core can be tolerated, we used optical ray tracing to calculate the effects of misalignments of the MLM elements.

Figure 5 shows the maximum acceptable displacement of the respective MLM key elements. The numbers in brackets denote how the specified maximum displacement will translate into displacement of the micropupil images on the fibres. At the moment, it is foreseen to use pinholes to couple the second lenslet array with the fiber interface plate. Hence, diameter and position of these pinholes must be very precise.

The total positioning error of the micropupils derives from the tolerances in brackets added in quadrature and stays well below 10 µm.

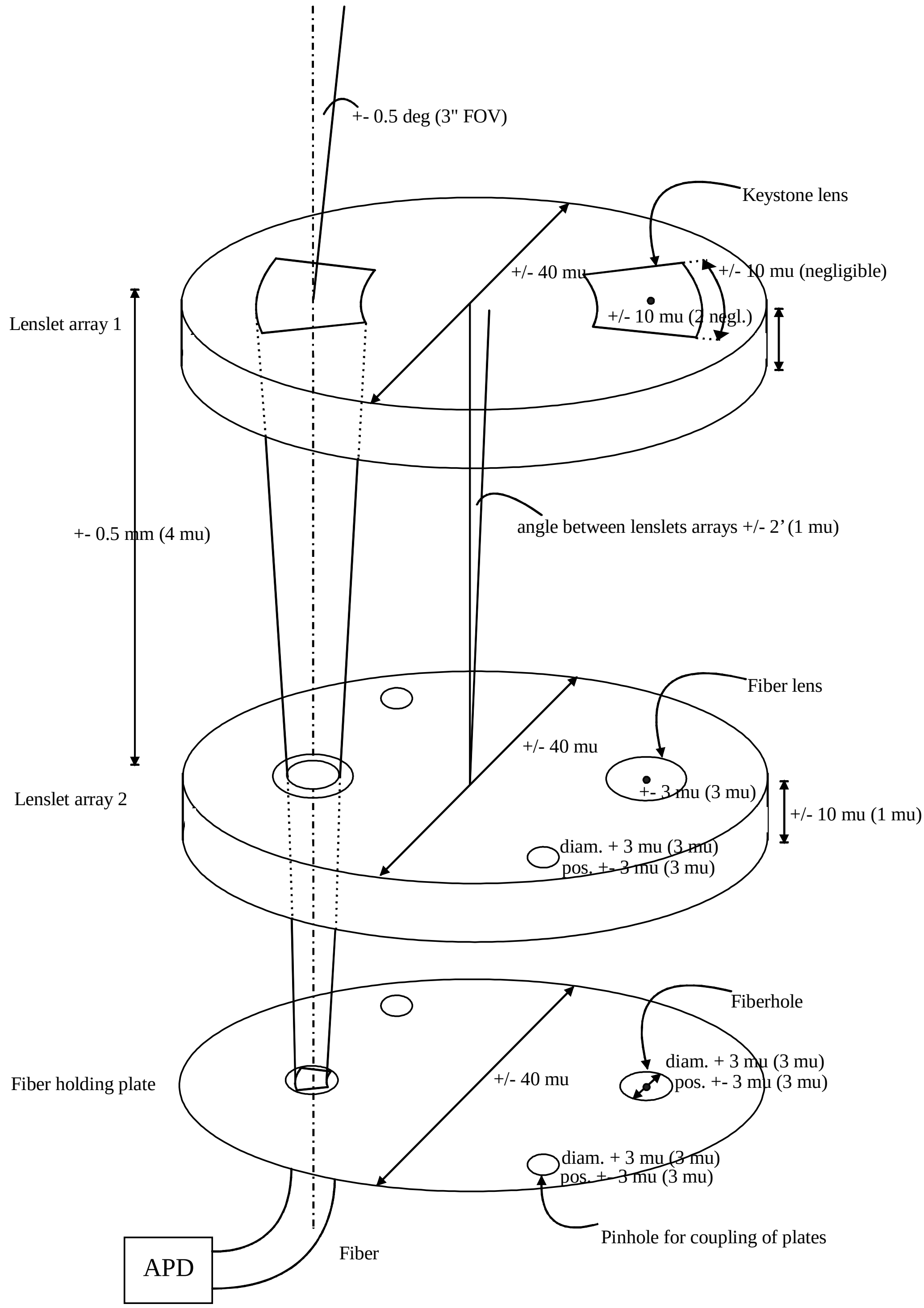

Figure 5: Lenslet array unit tolerances. Quantities in parenthesis denote displacement of micropupil with respect to fiber core.

Additional tolerances not shown in the drawing concern the concentricity of the fiber core with the fiber hole. Since it is foreseen to insert precise tubes into the fiber holes which guide the fibers, a number of quantities affect the precision in concentricity: concentricity of inner and outer boundaries of a tube, inner and outer diameter of a tube, concentricity of fiber core and cladding, and outer diameter of cladding.

According to fiber experts and tube specifications, the tolerance on every single of these five quantities is of the order of one micron. Hence, they add up to an additional error of about 3 μm rms.

6.2 Optical transmission

Here we consider losses ocurring at the transitions between materials of different refractive index and losses due to mis-alignment as discussed in the previous section.
The specification for each, the first and the second, lenslet array is 95% transmission (goal 97%) [RD8], i.e. the transmission at each coated surface is better than sqrt(0.95). There will be optical oil between the back-side of the 2nd lenslet array and the fibers, resulting in only one transition at the front-side of the 2nd lenslet array, and one transition (probably uncoated, i.e. ~ 95% transmission) at the fiber end. Hence, there are 4 transitions altogether (3 coated, 1 probably uncoated).
Suppliers claim that they can meet the tolerances given in the previous section based on our analysis. This ensures a positioning of the micropupils with respect to the fiber cores of better than 10μm, leading to an additional loss of light of 2% in the worst case.

Taking all these numbers into account, the overall optical transmission will be better than sqrt(0.95)^3 * 0.95 * 0.98 = 86%.

7 MECHANICAL ASSEMBLY

The mechanical assembly, called microlens module (MLM), consists of a front part containing the two lenslet arrays, a back part, caled fiber feed module (FFM), guiding and supporting the fibers, and an interface between the two. A detailed technical drawing of the MLM is attached to this document.

7.1 Fiber feed module

The FFM has been designed in order to satisfy the following important requirements:

- High precision in the positioning of the fibres
- High precision in keeping the fibers perpendicular to the holding plate
- High precision in the coupling between the fibres and the second lenslet array
- Minimise the possibility of fiber breakage, both during assembly and during normal use of the final system

To accomplish this, a “holding plate” for the fibers and some capillary tubes to guide the fibers in the mechanical housing are used.

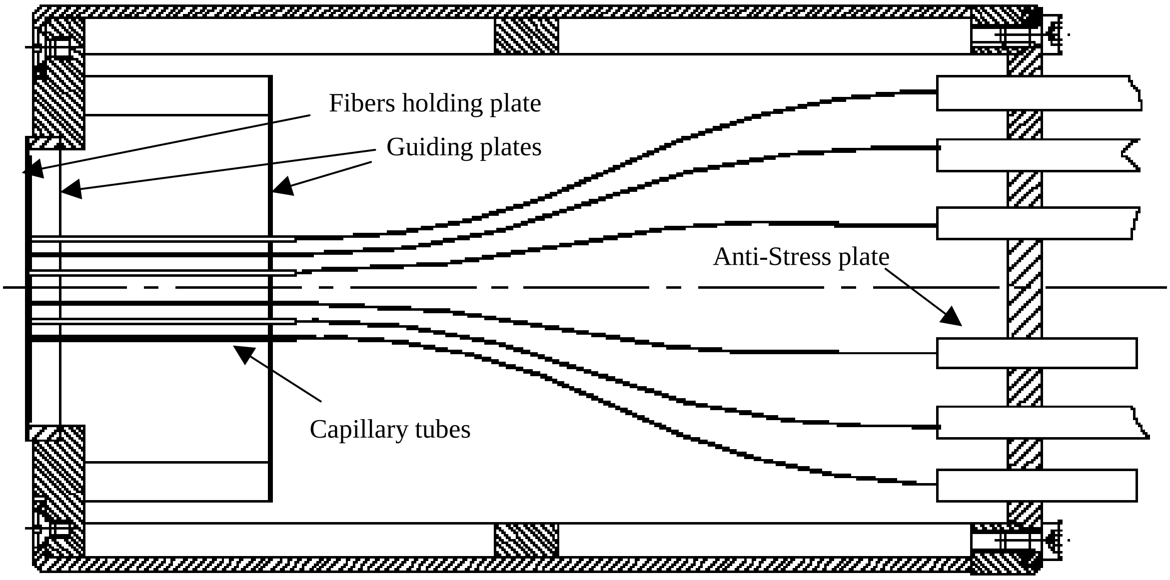

Figure 6: The fiber feed module

Main components of the fibers assembly housing (see Figure 6, a detailed technical drawing is attached to this document):

- On the left there is the **fibers holding plate**. This is a circular plate, 150 μm thick, made of Stainless Steel 1.4301, black, with 60 holes of the same diameter as the tubes at the micropupils' positions. Measurements on samples of these plates have been carried out in ESO laboratories and showed a very high accuracy in the holes' positions (maximum displacement and tolerance in the diameter of the order of 3 μm). The current plan foresees to couple the second lenslet array to the fiber holding plate by the use of interface pinholes.
- We decided to use **capillary tubes** to keep the fibers perpendicular to the holding plate and to guide them during insertion. These tubes are made of ceramic and very precise in terms of diameters and concentricity. They are maintained by two more guiding plates of the same precision as the fiber holding plate.
- On the right side there is another plate ("**anti-stress plate**") with 60 larger holes that interfaces with the external Kevlar protection of the fibers. The purpose of this plate is to give starin relief to the fibers.
- The **external housing** is made by two separated parts:
  1. a "framework like" black structure, which is holding all the plates, with large windows on the side to give access to the capillary tubes and the fibers during the assembly process
  2. an external protective and light tight cylinder, enclosing the complete system

Guidelines for the assembly process:

1. The fibers holding plate and the capillary tubes guiding plates will be mounted on the housing framework structure

2. The capillary tubes will be inserted and glued one by one in the two guiding plates
3. On one end of the fibers, a few centimeters of the plastic protection, and a few millimeters of the buffer will be removed.
4. The fibers with protection are inserted in the anti-stress plate
5. They are inserted through the capillary tubes without protection.
6. They are inserted into the holding plate without buffer and stopped by flat glass plate such that they are all at the same level.
7. The fibers will be glued in the capillary tubes
8. The anti-stress plate will be placed and screwed in the correct position and all the fibers protection will be attached to the holes
9. The external cylinder will be screwed to the framework structure

7.1.1 Optical fibres specifications

The following are the specifications concerning the optical fibres to be used for the lenslet array system.

Fibres type	Silica multimode
Fibres connector	One side: FC connector (goal: AR coated)
Fibres length	3 meters
Fibres core diameter	100µm
Numerical Aperture	0.22 - 0.35
Fibre cladding ratio	1.2 – 1.4
Transmission	Fresnel losses only
Core axis centering	± 2 µm

Table 1: Fibers Specifications

An optical fibre is normally composed of 4 different parts (see Figure 7):

- The **core**, which is the part where the light is propagated.
- The **cladding**, which is the external coating allowing the propagation of the light inside the core via total reflection; normally it is a lower refractive index optical material surrounding the core. The cladding thickness is normally specified as a ratio between the core diameter and the cladding diameter (a ratio 1.2 on a 100 µm fibre core means a final diameter core+cladding of 120 µm)
- The **buffer** is an outer coating, typically made of plastic material, and has the purpose to protect the fibre from external stresses or abrasion. It also gives the strength properties of the fibres once it is completely assembled. There are quite a number of different kinds of buffers, each of them giving different results is term of elasticity of the fibres and position accuracy between the buffer axis and the core axis
- External **protection**, which is normally a plastic or gummy material used with the only purpose to give the possibility to handle the fibre without damages

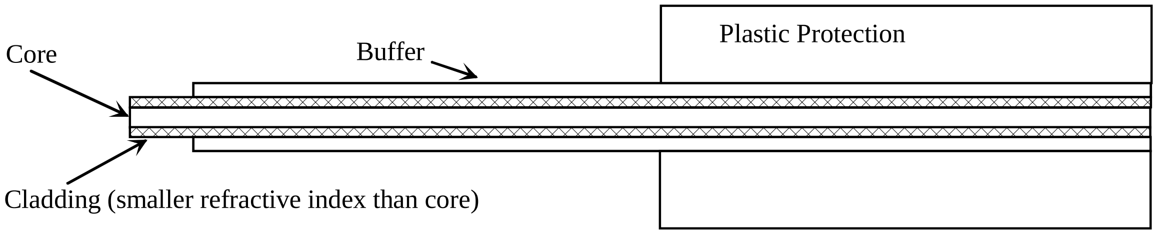

Figure 7. Fiber characteristics

7.2 Interfacing 2nd lenslet array and fiber plate

The interface consists of two high-presicion pins that allows us to achieve the required precision in alignment. As an alternative, precise reference crosses at the same positions on the lenslet arrays and on the fiber holding plate can be used for the alignment with a microscope. Optical oil will be put between the 2nd lenslet array and the fiber holding plate, so there is no transitions between materials of different refractive index here.

8 FIBER EXPERIMENTS

In order to prove that our concept of the MLM is working, we performed an experiment that resembles the situation for a single sub-aperture rather than all 60. In this context, we wanted to give answers to the following questions:

1. How much light gets lost by coupling the beam into the fibers using a second lenslet array (ball lens) to create micropupils on the fibers?
2. Would a larger core diameter, e.g. 125µm instead of 100µm, give us a better throughput to the APDs?
3. How sensitive is the light throughput to x- and y- displacements between the two lenslet arrays?

The set-up we used for the experiments is schematically displayed in Figure 8, and a picture is shown in Figure 9. A halogen lamp delivers a white spectrum that is coupled into a fiber. The end of this fiber serves as a point source located in the front focal plane of the collimating lens. The first lenslet is represented by a lens with a similar focal length (50 mm), which is obscured by a laser cut mask with exactly the same shape and size as the (larger) subapertures in the outer ring. The elements enclosed by the box as displayed in Figure 8, are all mounted on the same stage which allows us very precise adjustments of the order of 1 µm in the plane perpendicular to the beam. The second lenslet is represented by a ball lens of diameter 1.5 mm. The ends of the fibers feeding the APDs are glued at a position where the ball lens forms an image of the mask (this is critical and must be precise to a few µm's). A magnetic mount allows us to interchange different fibers, glued to their balls, with a very high precision of 1 µm.

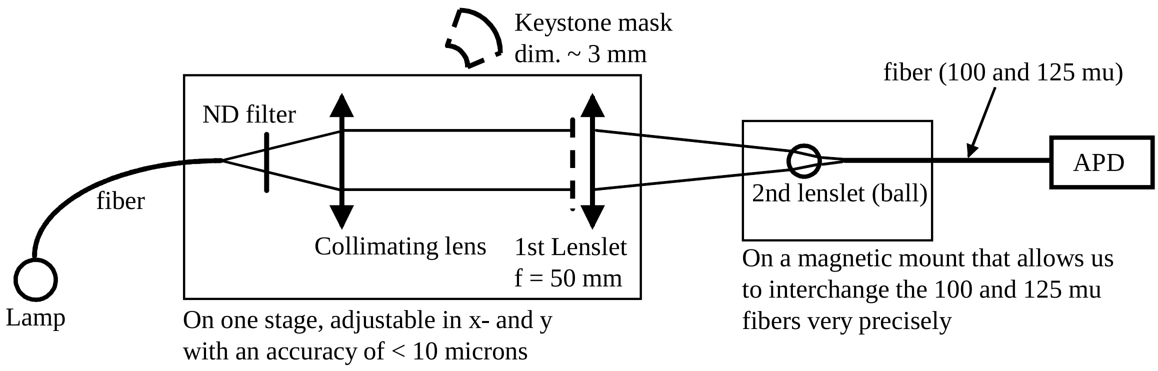

Figure 8: Schematic layout of the experiment to verify the MLM concept.

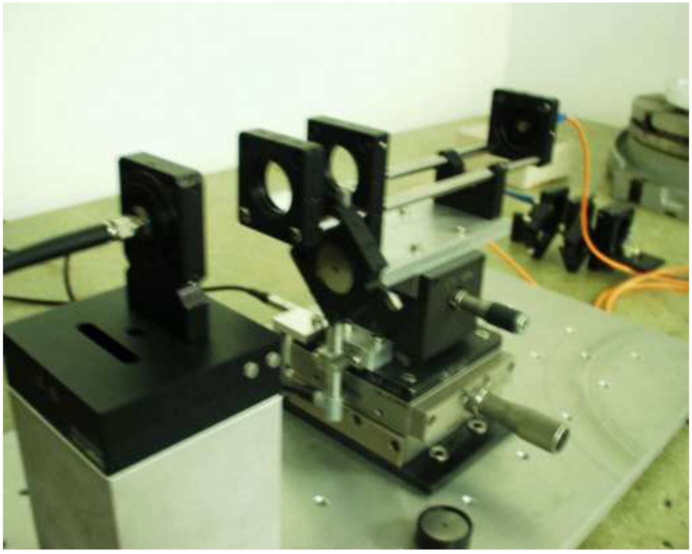

Figure 9. Picture of the experiment setup.

This set-up allows us to address the questions mentioned above by the following experiments:

8.1 Experiment 1: Coupling efficiency at fiber input

Measurements:

We measured the total flux at the position of the ball lens (P1) and at the FC connector (P2), i.e. before and after coupling the light into the fibers. For this purpose, we use a photodiode (not an APD) with a large sensitive area of several square millimetres that can easily be used to collect all the light at both locations. In order to avoid chromatic effects due to the different spectral sensitivity of the photodiode and the APDs, we insert a narrow band filter with a central wavelength matching the one where the APD is most sensitive. The difference in flux detected at the two positions tells us the loss of light due to the injection into the fibers. This was done for both fiber core diameters (100 and 125 μm).

Results:

Here are the results averaged over three measurements at each position and two different light levels. The background intensity in each case was negligible (~ 4 pW).

	Intensity at P1 [nW]	Intensity at at P2 [nW]	Throughput [%]
125 μm core	22.4	17.95	80.1
100 μm core	22.4	17.5	78.1

Discussion:

A throughput of about 80% is in perfect agreement with the expected losses of light at the four uncoated glass / air transitions of 5 – 6 %. The slightly worse efficiency of the 100μm core fiber may not be due to a decreased coupling efficiency for the smaller core, but to a small misalignment of this fiber with respect to its ball lens. Such a misalignment is indicated by the light distribution at the fiber exit, being wider and more asymmetric than for the 125μm fiber.

8.2 Experiment 2: Coupling efficiency at fiber output (APD)

It seems reasonable to assume that a larger fiber core diameter would relax the alignment requirements. However, we have to consider not only the light injected into the fiber, but also the light accepted by the APDs with their very small photosensitive area (~ 175 μm squared). Considering that the re-imaging lens inside the APD modules magnifies the image of the fiber core by factors of 1.25 at 400nm and 1.55 at 1μm wavelength, some loss of light using the 125 μm fiber can be expected at longer wavelengths.
Knowing the amount of light injected into the two fibers from experiment 1, we are able to determine how much light is lost in an APD module due to the different core diameters. After having found the position of maximum throughput (see next experiment), we measured the flux detected by a certain APD for both fibre diameters. We repeated the measurement using four different APD modules to study their individual properties. Here are the specifications of those modules given by Perkin Elmer:

APD #	Dark Counts [Hz]	Quantum efficiency at 550 nm
5735	60	63.5
6038	32	64.9
6052	20	66.7
6024	35	64.7

Combined with the results from experiment 1, we can determine the loss of light in the APD modules due to the larger (125 μm) core diameter.

Results:

Here are the results averaged over a few measurements for each fiber and the four different APD modules. The light level was kept constant during the experiment. The background intensity is subtracted.

APD #	Flux for 100µm fiber [kHz]	Flux for 125µm fiber [kHz]	Ratio
5735	848.3	769.5	1.10
6038	833.3	749.5	1.11
6052	765.3	721.5	1.06
6024	813.3	758.5	1.07

Discussion:

Even though the throughput of light through the 125µm core fiber is slightly higher, the APDs see 6 – 11 % more light from the 100µm fiber. This effect can be attributed to the image of the 125 µm core being larger than the sensitive area of the APDs (~175 µm according to Perkin-Elmer). Since the size of this area slighty differs with the diodes, the losses are different. Furthermore, the modules may vary in the lateral alignment of the APDs with respect to the fiber core axis defined by the FC-connector.
We also performed the measurements using a smaller mask (inner ring), and achieved the same results.

8.3 Experiment 3: Impact of misalignment between 1st and 2nd lenslet array

Here, we used the precisely adjustable mount for the elements enclosed by the left box in Figure 8. By moving this stage, i.e. creating a displacement between lenslet array 1 and 2, we measured the corresponding loss of light and found the positions of maximum throughput used during the previously explained experiment. This was done for both fiber diameters (100 and 125 µm) to evaluate a possible advantage in using the larger core ones.

Results:

Figure 10 and Figure 11 display the effect of introducing a lateral shift between the 1st and the 2nd lenslet array. The data were taken using APD5735.

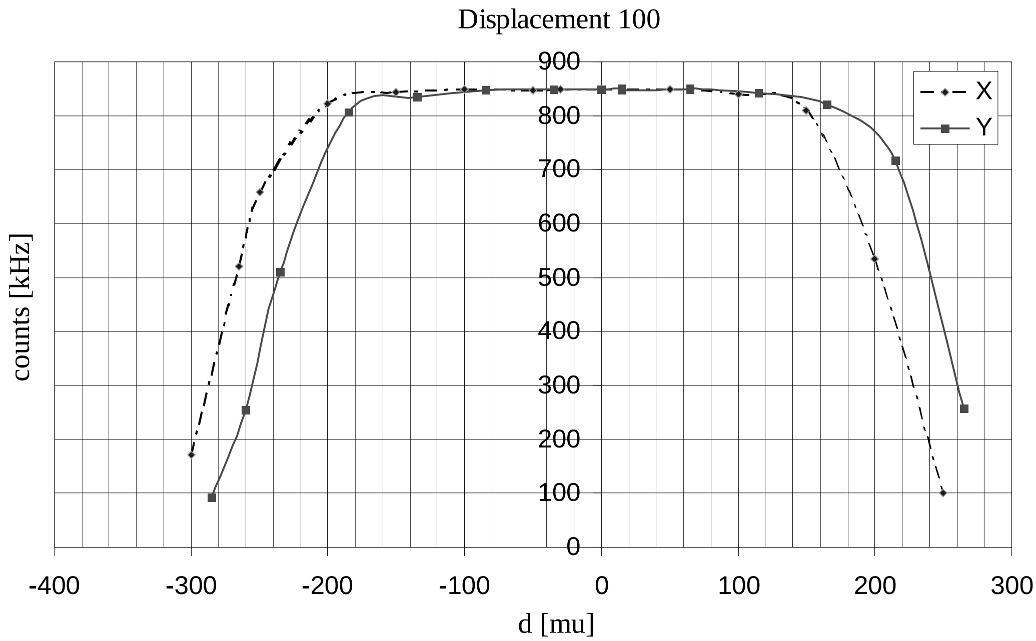

Figure 10. Signal versus displacement for the 100 μm fiber.

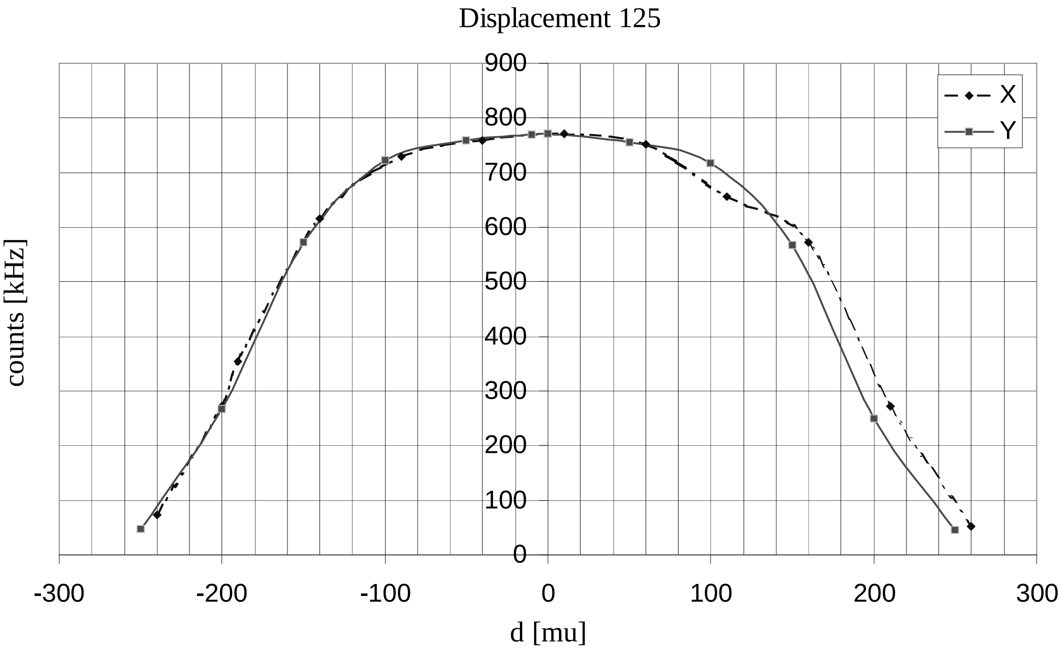

Figure 11. Signal versus displacement for the 125 μm fiber.

Discussion:

As shown in Figure 5, the effect of a lateral shift between the two lenslet arrays (displacement of one lenslet in the first array), should ideally be negligible (a 50 μm shift should introduce only ~1 μm shift of the image on the fiber). We see indeed, that shifts of

up to 100 μm do not lead to considerable losses of light. For the alignment, the value of 100 μm has to be shared between shifts and twisting of the two lenslet arrays. For example, a twisting of 0.8° causes a displacement of 100 μm for a lenslet in the array's outer ring. We attribute the severe losses for larger shifts to the non-ideal ball lens, introducing strong aberrations when used to far off-axis.
The 125 μm fiber suffers more from lateral shifts, a behavior we did not expect and do not fully understand at the moment.

8.4 Conclusions

The concept of coupling light into fibers by using a second lenslet array to reimage the first one onto the fiber entrance works. The losses of light are consistent with the unavoidable Fresnel losses at air/glass transitions. In the final system, there will be only two such transitions, at the (coated) 2nd lenslet array surface and at the fiber exit. In order to maximize the throughput, we should try to have the fiber exits at the FC-connector coated.
Using fibers with core diameters larger than 100 μm leads to severe light losses in the APD modules, because then their internal lenses cannot focus all the light onto the sensitive areas any more. However, the precision required with the 100 μm fibers is achievable by manual alignment of the fiber core with respect to a ball lens even for the large subapertures of the outer ring. Hence, the use of 100 μm fibers for the final system is suggested.

9 STATEMENT OF WORK

In the following, we report the status of the development of the lenslet array unit. The development actually involves three main parties:

Heptagon, Switzerland: This appears to be the only manufacturer of lenslet arrays who can fulfil our needs in terms of precision and optical quality. Heptagon will deliver the 1st and 2nd lenslet arrays. Currently, it is foreseen to order 12 arrays of both types in order to have a spare for each system. See **RD 10a** for technical specifications and statement of work

Optocomm, Heidelberg or Stygma Optique, Paris: Optocomm can deliver the optical fibers assembled with FC connectors on one side and precise ceramic tubes on the other side. They would also assemble the fiber housing, where the mechanical parts (plates, mechanical interface and frame) would be delivered by ESO (potential suppliers have already been identified). Stygma Optique could deliver the whole fiber housing including mechanics.
Both solutions appear feasible. A decision will be taken after having received detailed offers.

ESO: ESO will manufacture and assemble the mechanical part holding the two lenslet arrays and interface it with the fiber housing. See technical drawings of the lenslet array unit attached to this document.

10 MAINTENANCE

Since it will be difficult to repair the lenslet array unit (possible events: broken fibers or severe mis-alignment) without the expertice of the developpers, it is foreseen to have at least two permanent replacement units on Paranal. Due to the closed unit design, steady maintenance does not appear necessary.